UCLA
UCLA Electronic Theses and Dissertations

Title

The Design and Characterization of Elastin based Bioadhesive for Vascular Anastomosis

Permalink

https://escholarship.org/uc/item/2cx232rg

Author

Unal, Gokberk

Publication Date

2020

Peer reviewed|Thesis/dissertation

UNIVERSITY OF CALIFORNIA

Los Angeles

The Design and Characterization of

Elastin based Bioadhesive for

Vascular Anastomosis

A dissertation submitted in partial satisfaction of the

requirements for the degree Master of Science in

Chemical Engineering

by

Gokberk Unal

2020

ABSTRACT OF THE THESIS

The Design and Characterization of

Elastin based Bioadhesive for

Vascular Anastomosis

by

Gokberk Unal

Master of Science in Chemical Engineering

University of California, Los Angeles, 2020

Professor Nasim Annabi, Chair

Cerebrovascular ischemia from intracranial atherosclerosis remains difficult to treat. Current revascularization procedures, including intraluminal stents and extra cranial to intracranial bypass, have shown some benefit but are not without limitations due to high peri- and post-operative morbidity. We therefore developed a novel approach that involves gluing of arteries and subsequent transmural anastomosis from the healthy donor into the ischemic recipient. This approach required a new vascular sealant with distinct mechanical properties and adhesion which is not commercially available. We engineered an elastic glue based on functionalized elastin-like polypeptide (ELP) with methacryloyl groups (m-ELP) and fully characterized it *in vitro*. The

select formulation attained desirable mechanics (elastic modulus: 288 ± 19 kPa, extensibility: 34.5 ± 13.4 %), adhesion (shear strength: 26.7 ± 5.4 kPa), and biocompatibility (2D viability: 98 ± 1 %). In addition, testing in an *ex vivo* porcine anastomosis model achieved burst pressure of 34.0 ± 7.5 kPa, which is well over normal, elevated, and hypertensive crisis systolic blood pressures in humans at 16, 17.3, and 24 kPa respectively. Furthermore, a preliminary *in vivo* swine model assessed the feasibility of the two-glue sealant as well as the endovascular anastomosis application. The glue was applied and cross-linked at the anastomosis site under homeostatic conditions without difficulty. The anastomosis was created without bleeding complications and then confirmed by x-ray imaging. The procedure was well tolerated. Future studies will explore radio frequency ablation for creating the anastomosis, including how the hydrogel responds to temperature and humidity changes. Additional studies are needed to develop an algorithm to determine the size of the anastomosis unique to each patient. The formulation we developed is not limited in its uses. GelMA/m-ELP hydrogels can serve as sealants with remarkable elasticity and adhesion for vascular or pulmonary defects. Furthermore, the prepolymer solutions can be bioprinted or casted into functionalized scaffolds containing cells or drugs for tissue engineering and drug delivery systems.

The thesis of Gokberk Unal is approved.

Junyoung O. Park

Vasilios Manousiouthakis

Nasim Annabi, Committee Chair

University of California, Los Angeles

2020

Table of Contents

List of Figures

Acknowledgements

I would not be who I am today if it was not for the people around me. For that, I will forever be grateful. None of this would have been possible without my parents, Vuslat and Faruk Unal. I must admit that their vision, albeit I diverge from at times, has been the fundamental guide that none could match thus far in life.

Thanks to Selim Senkan, Yvonne Chen, Vasilios Manousiouthakis, Tim Grasel, Junyoung O. Park, and many other UCLA faculty for sharing their wisdom throughout my undergraduate and graduate years.

Thanks to Nasim Annabi, for accepting me as a Master's student and providing numerous opportunities.

Thanks to Jesse Jones, Naoki Kaneko, and Satoshi Tateshima for their valuable collaboration.

Thanks to all my fellow lab members, Ehsan for passing on his research skill, Senne for showing the path to selflessness.

Thank you Teresa for realizing my potential.

CHAPTER I. Background

When hematologic tissue perfusion fails to satisfy metabolic demand, resultant ischemia leads to eventual cell death. The most frequent clinical scenario demonstrating this pathophysiology is arterial stenosis upstream of the tissue capillary bed due to atherosclerosis (lipid deposition into the vessel lumen). Any organ supplied by such an arteriovenous circuit is susceptible, as evidenced by common ailments like stroke, myocardial infarction, and distal extremity gangrene. Current revascularization procedures including intraluminal stents and artery to artery bypass have shown some benefit, but are not without limitations [1-3]. Cerebral ischemia from intracranial atherosclerosis, in particular, remains difficult to treat. Stenting a diseased cerebral artery risks apposing plaque against small perforating branches and occluding them. Intracranial bypass is technically challenging and carries high preoperative morbidity, in part due to infarcts occurring while the recipient vessel is clamped and the anastomosis sutured in. We therefore sought to develop a novel bypass approach whereby clamp time may be eliminated. The proposed technique involves penetrating from donor artery to recipient using a small needle and then expanding the anastomosis. A would closure device such as a hydrogel-based sealant is required to appose the two vessels side by side, and maintain hemostasis around the circumference of the transluminal penetration zone.

Identifying the optimal device to secure the anastomosis site required a thorough evaluation of the its desired characteristics. Wound closure devices are utilized as physical barriers to minimize transport in or out of the operation site, ideally analogous to the healthy function of the native

tissue applied upon. Proper sealing is essential to prevent post-operative complications such as infections and dehiscence [4, 5]. The ideal wound closure device will maintain its structural integrity and mechanical stability under reasonable stress and changing environmental conditions to achieve such sealing capability. Additional desirable characteristics include biocompatibility and biodegradability to induce minimal hindrance to the natural wound healing process [6]. Sutures, staples, strips, and hydrogel-based sealants are devices that have distinct advantages and disadvantages.

Despite the emergence and rapid growth of hydrogel-based surgical sealants since early 2000s, sutures and staples are projected to continue dominating the wound closure market for the upcoming decade. This is largely due to the inferior mechanical strength, higher complexity, and cost of hydrogel-based sealants relative to their simpler, single-component counterparts. However, sutures and staples are not suitable for all applications. For example, novel sealants can simultaneously serve as scaffolds that encapsulate and regulate the controlled release of therapeutic drugs [7-9], as haemostatic or conductive patches [10, 11], as cellular transports [12]. Furthermore, internal organs such as the lungs, bladder, diaphragm, and blood vessels undergo significant changes in volume throughout their normal functions. Wounds on such organs carry increased risk of failure when closed with sutures and staples because they have dissimilar mechanical properties to the native tissue [13]. Therefore, we decided to use a hydrogel-based sealant for the proposed application.

2

There are several vascular sealants currently available. Poly(glycerol sebacate) acrylate based SETALIUM™ and bovine serum albumin-glutaraldehyde based BioGlue® are vascular sealants that have been shown to achieve hemostasis without thrombus formation or stenosis in carotid artery and jugular vein defects in a porcine model [14, 15]. There are also a number of fibrin based natural sealants that are used to strengthen vascular suture lines [16]. Although these sealants are designed to promote coagulation while maintaining biocompatibility and biodegradability, mechanical characteristics do not appear to be amongst the primary design parameters. The proposed anastomosis requires a novel elastic vascular sealant that, unlike others, is not readily hemostatic. We have thus begun designing a specialized hydrogel-glue.

A wide range of synthetic and natural polymers have been used to formulate hydrogel-based sealants for different medical applications [17]. Some prominent examples of synthetic polymers include poly(ethylene oxide) as a surgical adhesive [18], poly(vinyl alcohol) as a hydrogel matrix for cartilage regeneration [19], and polycaprolactone as a barrier for post-operative adhesion [20]. Synthetic polymers are associated with low production costs, are easy to apply, and have low risk of triggering an immunogenic response. However, poor cell infiltration and potentially toxic degradation by-products limit their use to cutaneous applications. On the other hand, natural polymers that are used in surgical sealants include polysaccharides (hyaluronic acid, alginate, chitosan, etc) and polypeptides (collagen, fibroin, elastin, fibrin, etc). Polysaccharides are biocompatible, biodegradable, and can exhibit antimicrobial properties. Protein-based hydrogels have increased tendency to trigger an immunogenic response by the host [21];

however, their unique adhesion, tunable properties, and stimuli responsiveness make them ideal materials for tissue sealant applications.

The two natural polymers used in this study are gelatin methacryloyl (GelMA), a functionalized derivative of collagen, and methacryloylated elastin-like-polypeptide (m-ELP), a 365-aa recombinant elastomer designed to mimic the properties of natural elastin. Previous works demonstrate photocross-linking of ELP hydrogels through disulfide bond formation [22]. However, ELP by itself is not capable of forming a stable enough hydrogel with sufficient mechanical characteristics to serve as a surgical sealant. Methacryloyl functionalization is used to increase the degree of cross-linking of various synthetic and natural polymers through the addition of reactive terminal alkene residues that are capable of forming covalent linkages between proximal chains in the presence of an appropriate catalyst and light source. Therefore, we have functionalized the lysine, serine, and tyrosine residues on ELP with methacrylamide and methacrylate groups respectively to obtain m-ELP, an elastomer capable of forming a stable hydrogel standalone via covalent bonds. GelMA and m-ELP were combined in an Eosin-Y based, visible-light-activated photoinitiator system to form a composite formulation.

In this study, we report molecular and mechanical characterization, *ex vivo* adhesion tests, *in vitro* cytocompatibility analysis, and two *in vivo* experiments. The goal is to take advantage of the high adhesion of GelMA and elasticity of m-ELP to develop a potent vascular sealant capable of enduring hypertensive crisis blood pressures (24 kPa, 180 mmHg) for the proposed application of anastomosis in cerebrovascular ischemia.

CHAPTER II. Materials and Methods

Synthesis of GelMA

GelMA was synthesized as explained previously [23]. In short, gelatin from cold water fish skin was dissolved in DPBS (10% w/v). Then, methacrylic anhydride was added dropwise (8% v/v) at 60°C and the mixture was allowed to react for 3 h under continuous stirring. The reaction was then stopped by 1:4 dilution in DPBS. Finally, the solution was dialyzed against deionized water for 7 d, frozen at -80°C for 2 h, and desiccated for 5 d to yield high GelMA (~80% methacryloylation).

Synthesis of m-ELP

Plasmid inserted, kanamycin resistant E. coli strain genetically modified to encode ELP was removed from -80℃ storage and inoculated in 10 mL LB Broth. The starter culture was left overnight in a shaker incubator at 37℃, 190 rpm. The starter culture was then transferred into 1.5 L Terrific Broth containing kanamycin (50 mg/L) and placed back in the shaker incubator for 24 hours. The liquid culture was then centrifuged at room temperature, at 17000x g for 20 minutes. The pellet was collected, placed in lysis buffer (5.84 g-NaCl/L, 0.48 g-MgCl$_2$/L, 1.00 mL-βME/L in (1x) TE Buffer) at 4℃, and kept in the refrigerator overnight. The mixture was then sonicated and refrigerated overnight. Inverse transition cycling was applied with one cycle of cold and warm spin per day for four days. After the fifth cold spin, the solution was pipetted into dialysis membranes and dialyzed against milli-Q water (changed twice per day) at 4℃ for 4 days. The purified solution was frozen at -80℃ and lyophilized to yield ELP.

ELP was dissolved in 4℃ PBS (10% w/v) and methacrylic anhydride was added dropwise to a 15% v/v final concentration. The mixture was continuously stirred in ice bath and was allowed to react for 16 hours. The mixture was then diluted into 4x volume with cold PBS and dialyzed in a dialysis cassette against milli-Q water (changed twice per day) at 4℃ for 4 days. The purified solution was frozen at -80℃ and lyophilized to yield m-ELP.

NMR Analysis

There are well-established methods to determine the degree of methacryloyl functionalization of the extensively studied polymers such as GelMA, which involves the quantification of the diminishing free lysine H-NMR signals with increasing degree of methacryloylation [24, 25]. Here, we had to develop a new strategy to identify the molecular characteristics of m-ELP because of (i) the low lysine content of ELP (2 per chain) and (ii) the high hydroxyl to amine residue ratio throughout the peptide sequence (serine and tyrosine : lysine). Similar studies for other polymers include the use of a reference molecule. We employed this approach and used PEG-2000 (Sigma, CAS: 25322-68-3) as our reference molecule to derive the following equation for a generic degree of methacryloylation, which can be used separately for methacrylamide functionalization (of lysine) and methacrylate functionalization (of serine and tyrosine).

$$\% \text{ Methacryloylation} = \frac{\int (H^* + H^{*\prime})}{\int (\text{PEG})} \cdot \frac{n_{PEG}}{n_{m-ELP}} \cdot \frac{1}{\Psi} \cdot \frac{179 H_{PEG}}{2 H^*_{m-ELP}}$$

The H* and H*' are the two terminal alkene protons that present two distinct singlets of exactly the same intensity at slightly different chemical shifts due to stereochemistry around the alkene. The terms n_{PEG} and n_{m-ELP} are the controlled number of moles of PEG and m-ELP respectively in the NMR sample. Ψ is the number of relevant residues per ELP chain; for methacrylamide functionalization, $\Psi = 2$ (2 lysine residues in sequence) and for methacrylate functionalization, $\Psi = 9$ (5 serine and 4 tyrosine residues in sequence). The constant in the last term is factored in to normalize the H-NMR signal intensities as there are 179 protons that contribute to the PEG peak at 3.47 ppm and a total of two protons that contribute to the aforementioned H* and H*' peaks.

Bioadhesive Formation

Two photoinitiator stock solutions were prepared. The TEOA-VC stock was prepared by dissolving triethanolamine (TEOA, 3.75% w/v) and N-vinylcaprolactam (VC, 2.5% w/v) in PBS. The second stock contained 1 mM Eosin Y in PBS. Both stocks were kept in dark at 4℃. TEOA-VC and Eosin Y stocks were mixed at 4:1 ratio respectively to obtain active photo-initiator solution. Composite prepolymer solutions were prepared by adding 30:0, 20:10, 15:15, 10:20, 0:30 GelMA:m-ELP ratios to achieve 30% (w/v) total polymer concentration. The active photo-initiator solution was first cooled to 15°C. The m-ELP was added and vortexed (3000 RPM) at 15°C for 30 minutes until dissolved. Lastly, GelMA was added and vortexed (3000 RPM) at 15°C until dissolved. Solutions were vortexed continuously until further use. Cross-linking is achieved by visible light exposure with wavelength of 450-500 nm (FocalSeal Xenon, Genzyme, 100 mW/cm^2) for 160 seconds.

Mechanical and Rheological Properties

The composite prepolymer solutions were pipetted into polydimethylsiloxane (PDMS) molds of rectangular geometry (12 x 4.5 x 1 mm) for tensile testing and of cylindrical geometry (d: 5 mm, h: 4 mm) for cyclic compression testing and cross-linked.

Tensile Test: The two ends of the rectangular hydrogel samples were placed between transparent, double sided, adhesive polyethylene terephthalate (PET) sheets and loaded to an Instron 5542 mechanical tester with tensile grips installed. The hydrogel samples were then stretched longitudinally at a rate of 1 mm/min, and tensile strain (%) and tensile stress (kPa) were measured with BlueHill Universal software. The extensibility percentage was determined by maximum strain and the Young's Modulus was obtained by calculating the slope of stress versus strain plots for each sample.

Unconfined Cyclic Compression Test: The cylindrical hydrogel samples were placed between the compression grips of an Instron 5542 mechanical tester. The grips were manually brought closer together until the hydrogel sample was under zero strain, barely in contact with the top grip. The sample was then compressed and decompressed for 10 cycles to a maximum of 40% strain, at a rate of 5 mm/min. Compressive strain (%) and stress (kPa) were measured with BlueHill Universal software. The unconfined compressive modulus was determined from the slope of the initial linear region of cycle 1 stress versus strain compression curve. The energy loss percentage was calculated by taking the difference between the integral of the compression and the decompression stress versus strain curves for each cycle.

8

<u>Swelling Test:</u> Cylindrical samples were weighed (0 h) and placed in 1 mL phosphate buffered saline (PBS) in separate wells of a 24-well plate. The samples were weighed at 2, 4, 16, 24, 48 hour intervals with fresh PBS added every interval.

$$\text{Deswelling Ratio}_{t=t_i} = \frac{w_{t_i}}{w_0}$$

<u>Degradation Test:</u> The samples were weighed (0 d) and placed in 1 mL of 20 µg/mL-PBS collagenase type II solution. The samples were weighed at 1, 2, 3, 5, 7 day intervals with fresh collagenase solution added every interval.

$$\%\text{Degradation}_{t=t_i} = \frac{w_0 - w_{t_i}}{w_0} \cdot 100\%$$

<u>Rheology</u>

Oscillatory rheology measurements were carried out on Anton Paar (MCR 302) by using a cone plate (radius 8mm, cone angle 2°). A solvent trap was used to minimize water evaporation during measurement. Temperature sweeps were performed from 5 to 40 °C at a heating rate of 1°C/min. For all measurements a frequency of 1 Hz and a strain of 1% were applied. This strain and frequency were previously determined to be within the linear viscoelastic region of these polymer solutions.

***In vitro* adhesion tests**

Burst Pressure Test: 40 µL of prepolymer solution was injected and cross-linked on a 1-mm in diameter hole made on collagen sheet seal (Appendix A1). Air was pumped at a rate of 10 mL/min using a syringe pump and the pressure inside the seal was measured using a PASCO wireless pressure sensor and software until the gel adhesion failed and burst.

Wound Closure Test: Porcine lung was cut in 3 x 1 x 0.5 cm pieces and glued longitudinally on glass slides with a 0.5 cm overhang in length. Two opposing pieces were then pushed together and 100 µL of prepolymer solution was injected and cross-linked on 1 x 1 cm combined overhang (Appendix A2). The slides were loaded to Instron 5542 Mechanical Tester with tensile grips and pulled apart at a rate of 1 mm/min. Tensile stress (kPa) was measured with BlueHill Universal software. Adhesive strength was taken to be the maximum stress, which also corresponds to the breaking point.

Lap Shear Test: Porcine arteries (5 mm collapsed width) were cut into 20 mm long segments and glued on glass slides. Prepolymer solution was applied on half of one segment (10 x 5 mm), over which the second segment was placed (Appendix A3). After cross-linking, the thickness of the hydrogel was measured with a digital caliper and the glass slides were loaded to Instron 5542 Mechanical Tester with tensile grips and pulled apart at a rate of 1 mm/min. Shear stress (kPa) was measured with BlueHill Universal software. Shear strength was taken to be the maximum stress at which the two artery segments were separated.

***Ex vivo* tests using a porcine anastomosis model**

Porcine carotid arteries prepared by removal of the tunica adventitia. Segments approximately 5 cm in length without branching were cut from parent vessel. In the first iteration of gluing, the prepolymer solution was injected directly in between two segments and cross-linked. Then, an anastomosis was made with an 18-gauge needle from the donor artery to the recipient. In the second round of gluing, the prepolymer solution was injected on both sides of the interface between the two segments and cross-linked to strengthen the anastomosis site. Both ends of the recipient artery and one end of the donor artery were ligated with suture. The open end was connected to a syringe pump. Saline solution (9 g-NaCl/L-H_2O) at 37°C was pumped at a rate of 4 mL/min and the pressure profile within the artery was measured using a PASCO wireless pressure sensor and software until the gel failed and the anastomosis burst.

***In vitro* cytotoxicity test**

Cell Line

Human umbilical vein endothelial cells (HUVECs) were chosen for the cytotoxicity studies of the prepolymer solutions because it is essential to evaluate the *in vitro* cytotoxicity of biomaterials with cells relevant to their particular application. In the case of a surgical sealant to be used for an inter-arterial anastomosis, HUVECs present as ideal candidates as such. Cells were cultured in Lonza EBM™ Basal Medium (CC-3121) with EGM™ Endothelial Cell Growth Medium SingleQuots™ Supplements (CC-4133).

2D cell seeding

Glass slides were cut in 1 cm² squares and coated with (trimethoxysilyl)propyl methacrylate (TMSPMA) to prevent hydrogel detachment for the entirety of the study. 10 µL of prepolymer solution was injected on a petri dish. The coated glass slides were placed over the drops of injected prepolymer solutions with a 150 µm spacer and the solutions were cross-linked for 30 s. The hydrogel-covered glass slides were then placed in separate wells of a 48-well plate with the gel facing up. 40 µL of cell solution containing 10,000 cells (250,000 cell/1 mL-media) was pipetted onto the hydrogel surface, then incubated for 30 min at 37°C. After the initial incubation, 1 mL media was added to each well and the samples were further incubated for 24 h. 2D cultures were maintained at 37°C in a 5% CO_2 humidified atmosphere. The culture medium was replaced every 48 h.

Cell Proliferation

PrestoBlue is an inherently non-fluorescent dye that becomes fluorescent when reduced through redox reactions, such as when exposed to the reducing environments around proliferating cells. The level of fluorescence is thus used to quantify cell proliferation. 10% v/v PrestoBlue solution was prepared in PBS under minimal light. Media was removed from the previously seeded samples (n = 5) 24 hours after seeding and 400 µL PrestoBlue solution was added. The samples were then incubated at 37°C for 45 min to promote cell attachment. After incubation, the reduced PrestoBlue solutions were transferred to separate wells of a 96-well plate and their absorbance values were measured with a plate reader on days 1, 4, 7 post-seeding.

Cell Viability

Live/Dead Cytotoxicity Kit (ThermoFisher) was used to evaluate cell viability. The cell-permeant green dye turns fluorescent after interaction with intracellular esterases of living cells and the cell-impermeant red dye turns fluorescent after binding to the DNA of cells that had undergone apoptosis. A composite dye solution containing 5 µL/10 mL green dye and 20 µL/10 mL red dye was prepared. For each time point after seeding (days 1, 4, 7), 330 µL of the composite dye solution was added to each sample (n = 3), which were then incubated for 30 min. After incubation, the dye solution was removed, and 1 mL PBS was added to each sample. The samples were imaged using a fluorescence microscope (Zeiss Axio Observer).

In vivo Studies

The *in vivo* behavior of the formulated hydrogels was investigated through two distinct animal models. First, the *in vivo* degradation profile and the biocompatibility were studied with a rat subcutaneous model. Then, the practicality of the glue and the proposed application was tested on a pig non-survival anastomosis model.

Rat subcutaneous model

Cylindrical hydrogel samples were prepared as described previously in Section of Mechanical and Rheological Properties. The samples were weighed, lyophilized for 24 h, and weighed again. Afterwards, the lyophilized samples were sterilized via exposure to UV light for 10 min. Dorsal pockets (8 mm) were created along the rats' backs and the samples were subcutaneously implanted. The animals carrying unique hydrogel implants were euthanized on days 7, 28, 56.

The samples were explanted and randomly assigned to be used for histopathological or degradation analyses.

Biodegradation Profile: The samples (n = 3) were carefully cleaned to remove any surrounding tissue and weighed. The *in vivo* degradation profile was then obtained similarly to the *in vitro* counterpart.

Immuno-Histological Analysis: The samples with intact tissue were fixed in 4% v/v paraformaldehyde solution in PBS for 4 h at 4°C. After fixation, they were soaked first in 10% for 4 h, then in 30% w/v sucrose solution in PBS for 24 h at 4°C. The samples were then flash-frozen in O.C.T. compound (Fisher) using liquid nitrogen. The blocks were sectioned into 10 μm thick slices using a cryostat (Leica CM1950). Samples from both groups were used in (i) hematoxylin/eosin (n = 3), (ii) CD3/DAPI (n = 3), and (iii) CD68/DAPI (n = 3) staining. The detailed protocol for the hematoxylin/eosin staining can be found here [26]. Anti-CD3 antibody (ab5690 - Abcam) and Anti-CD68 antibody (ab125212 - Abcam) were used as primary antibodies with AlexaFluor® 488 goat anti-rabbit (IgG) secondary antibody (ab150077) in accordance with the manufacturer protocols. The samples were then imaged using an inverted fluorescence microscope (Zeiss Axio Observer Z7).

Pig non-survival anastomosis model

The endovascular bypass was performed in swine (50-140 lbs, n = 4) under general anesthesia. The right common carotid and ascending cervical arteries were then surgically exposed, cleaned

of adventitia, and loosely looped with 3-0 silk through a para-midline linear skin incision. Topical papaverine hydrochloride was applied to the exposed arteries for vasodilation. The two arteries were placed closely in parallel. The prepolymer solution was applied directly to the arteries and cross-linked. Percutaneous arterial access was then obtained by femoral artery puncture. 100 IU/kg heparin was administered IV. Then, the femoral artery sheath was entered with an Outback re-entry catheter (Cordis, Bridgewater, New Jersey, USA), which was advanced to the carotid artery under fluoroscopic guidance. The Outback re-entry needle was deployed through the walls of both the carotid and ascending cervical arteries and a 0.014-inch Transcend guidewire (Stryker Neurovascular, Fremont, California) advanced coaxially into the recipient vessel. The anastomosis was subsequently dilated with a Gateway angioplasty balloon and finally a Wingspan stent (Stryker Neurovascular) was placed.

Statistical Analysis

Unpaired, one-tailed Welch's t-test was employed with a 95% confidence interval with a minimum of n = 3 samples for each test.

CHAPTER III. Results and Discussion

H-NMR data highlights the emergence of the methacrylate (α/β) and the methacrylamide (γ/δ) proton peaks for m-ELP (Figure 1, c-d) within 5.2-5.7 ppm range. Knowing the stoichiometric amounts of lysine, methionine, serine, and threonine residues, we used a reference molecule to determine the percentages of modified amino acids. H-NMR analysis of m-ELP has shown 40% degree of methacryloyl functionalization of lysine and terminal methionine amines to form methacrylamide groups and 8% degree of methacryloyl functionalization of serine and threonine residues to form methacrylate groups. These values are in agreement with the degree of methacryloylation of tropoelastin to yield MeTro following the same synthesis method. Similarly, the degree of methacrylamide functionalization for high GelMA was quantified to be 82%, which is in agreement with the previously published results following similar synthesis protocols.

Preliminary assessment was performed on composite prepolymer solutions containing varying total polymer concentrations (15, 20, 25, 30, 35% w/v) and GelMA:m-ELP ratios (0:100, 25:75, 50:50, 75:25, 100:0). Based on this, we decided to proceed with the 30% w/v total polymer concentration composites because (i) it had been shown by our previous work [27] that increased total polymer concentration correlated with enhanced mechanical properties and lowered degradation rate, both of which are desired for the proposed application, and (ii) qualitative assessment has shown that going over 30% w/v total polymer concentration in prepolymer solutions containing m-ELP is impractical due to their low solubility and injectability.
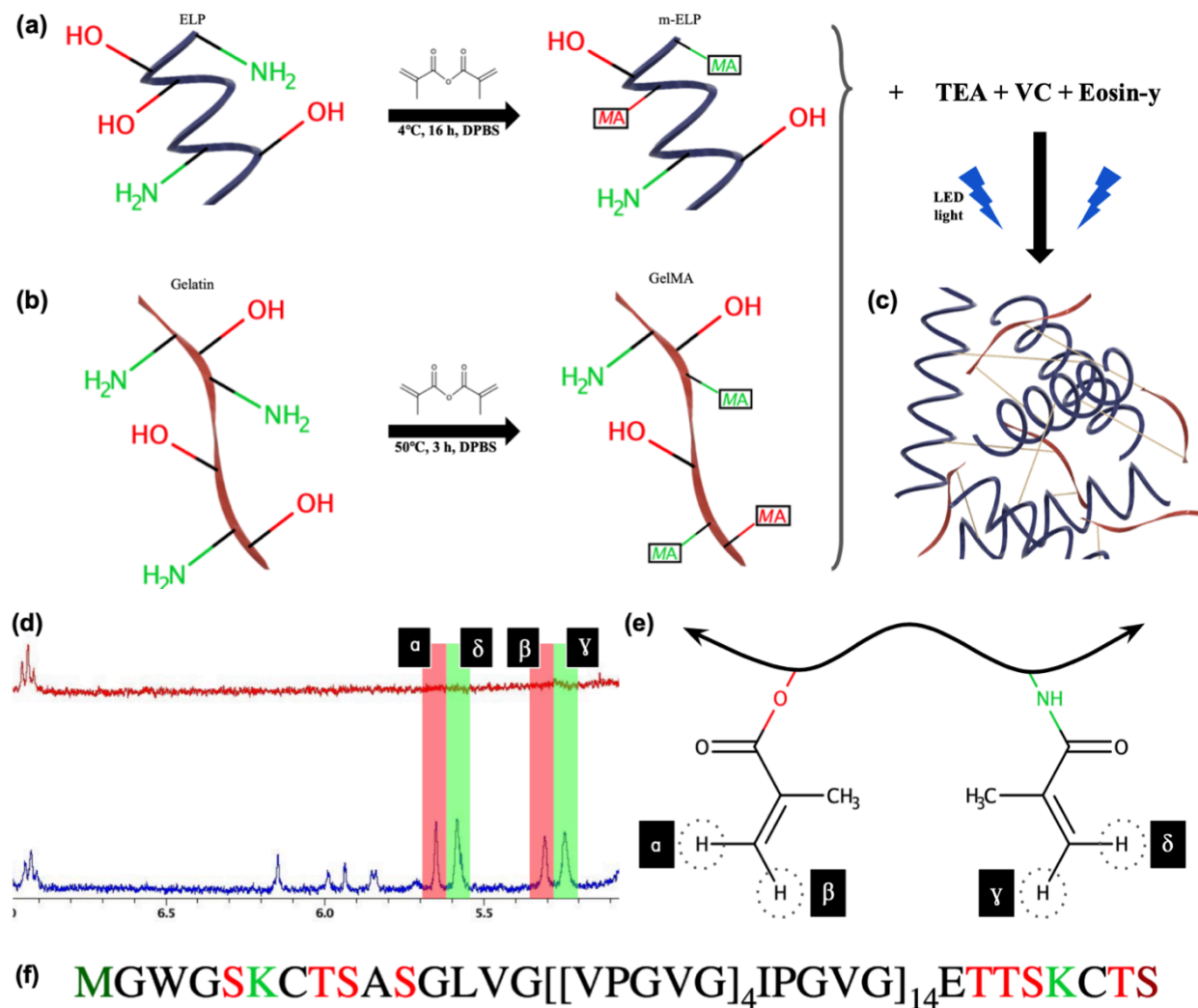
Fig. 1. Molecular characterization of methacryloyl functionalized gelatin and ELP polymers. **(a)** Methacryloyl functionalization reaction of ELP to yield m-ELP produces comparable amounts of methacrylate and methacrylamide groups. The m-ELP polymer has 55% methacrylamidation of primary amine groups of lysine and N-terminal methionine residues of the original polymer. Similarly, m-ELP has 8% methacrylation of hydroxyl groups of the serine and threonine residues of ELP. **(b)** Methacryloyl functionalization of gelatin to produce high GelMA preferentially modifies the lysine primary amines yields 82% methacrylamidation. **(c)** The polymers are dissolved in photo initiator solutions to prepare prepolymer solutions. The prepolymer solutions form composite hydrogels when irradiated with visible light through the formation of covalent linkages between methacryloyl groups. **(d)** H-NMR data of ELP (red) and of m-ELP (blue) confirms the modification of the original polymer. **(e)** Each of the two characteristic protons of both methacrylate and methacrylamide groups are labeled as shown on the H-NMR data. **(f)** ELP sequence. The lysine (light green) and the N-terminal methionine (dark green) residues have primary amine (-NH$_2$) groups that allow methacrylamide functionalization. The serine and threonine residues (red) have hydroxyl (-OH) groups that allow methacrylate functionalization. The C-terminal serine (dark red) has two potential methacrylation sites.

17

The initial approach was to optimize a formulation and use a single glue for the anastomosis site. This formulation would be chosen after a thorough systematic evaluation of mechanical properties, swelling and degradation profiles, and *in vitro* adhesion tests. The mechanical properties of hydrogels with varying GelMA:m-ELP ratios were characterized (Figure 2, a-d). Increasing GelMA:m-ELP ratio corresponded to enhanced Young's Modulus with a maximum of 581 ± 51 kPa in the pure GelMA sample, significantly greater than the next highest 319 ± 28 kPa in the 20:10 composite (p = 0.0004). The unconfined compressive moduli of the composite hydrogels increased significantly between each condition from 4 ± 3 kPa to 119 ± 14 kPa by changing the ratio of GelMA/m-ELP from 0/30 to 30/0. The pure GelMA sample also presented the smallest energy loss percentage at 4.8 ± 0.8 % after ten cycles of compression, followed by the 20:10 composite at 7.8 ± 2.2 %, and significantly less than the 15:15 composite at 15.4 ± 4.1 % (p = 0.022). The extensibility of hydrogel samples improved from 14 ± 2 % to 172 ± 17 % with increasing m-ELP concentration, as expected. Prior works demonstrate similar results for hydrogels containing ELP at 163 ± 11 % for hydrogels containing 15% w/v ELP [28]. The pure m-ELP sample could extend to almost three times its original size at 172 ± 17 % extensibility; however, although four of the five prepolymer solutions were injectable, the pure m-ELP solution was too viscous to be pipetted and thus presented itself impractical for a clinical setting. Still, incorporation of m-ELP in the composites made a significant contribution to the elasticity of the hydrogel even for the equivalent weight formulation (15/15%) at 35 ± 13 % extensibility. This allowed the vascular glue to be penetrable, and thus maintain its structural integrity post-anastomosis.

While the pure m-ELP sample had the lowest degradation at 14 ± 3 % after seven days in the collagenase type II solution, the composites degraded more than the pure GelMA gel. In other words, the degradation profile was at maximum at a GelMA:m-ELP ratio of 1, and decreased as the ratio diverged from 1 (Figure 2, e). The *in vitro* swelling test showed that all samples in fact shrunk in saline solution at 37°C (Figure 2, f). This was the expected behavior for both polymers. Previous works have shown that the swelling decreased with increased total polymer concentrations for hydrogels containing GelMA, and the swelling ratio approached zero at 20% total polymer concentration [29]. On the other hand, m-ELP is a temperature-responsive polymer and shrinks in elevated temperatures. Due to the temperature-responsiveness of m-ELP, a temperature dependent viscosity analysis was performed for solely practical purposes and the ideal operating temperature of the selected prepolymer solutions was determined to be between 15-18°C (Figure 2, g).

The adhesive properties of hydrogels were initially characterized using an *in vitro* burst pressure test on collagen sheet and a wound closure test on native porcine skin (Figure 3, a-b). The adhesion strength increased from 14.6 ± 0.8 kPa to 25.0 ± 1.4 kPa when the GelMA/m-ELP ratio was changed from 15/15 to 30/0. Adhesion to collagen sheet greatly improved with increased GelMA:m-ELP ratios and the pure GelMA sample achieved 25.0 ± 1.4 kPa (~190 mmHg), which was promising as the systolic blood pressure during hypertensive crisis is 180 mmHg. On the other hand, there was no significant difference in adhesion to native porcine skin between the different formulations. Following the previously mentioned initial approach of using a single-glue system and the observed mechanical and adhesive properties of different
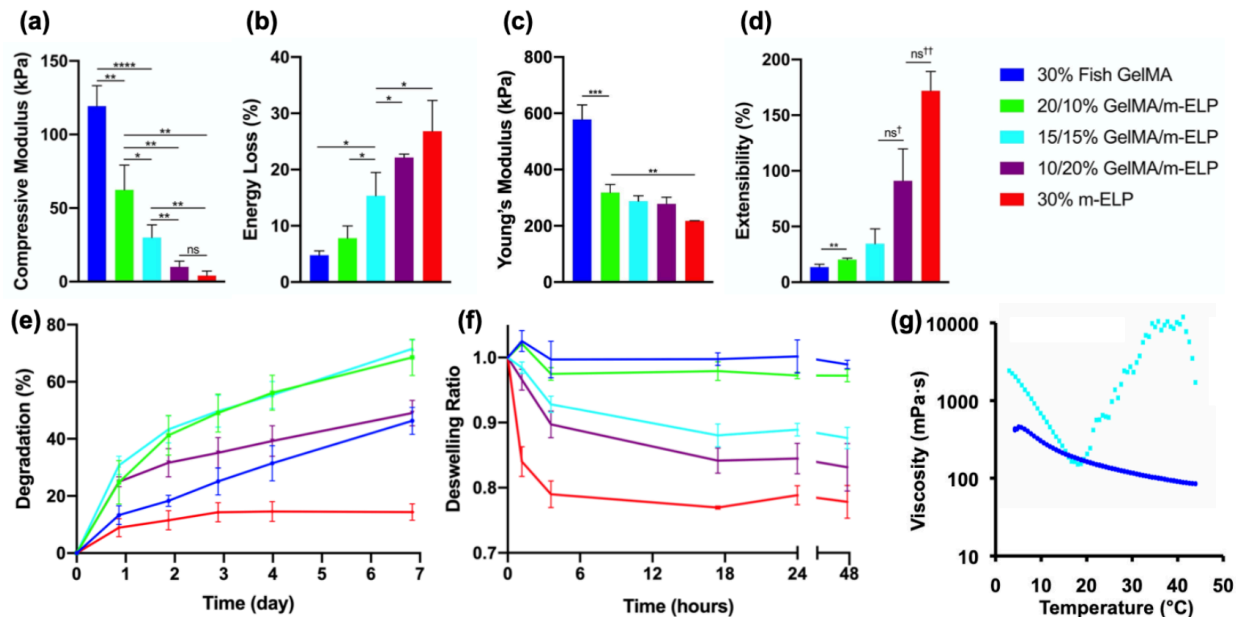
19

Fig. 2. Mechanical characterization of composite GelMA/m-ELP hydrogels. (a) Compressive modulus and **(b)** energy loss percentage of composite hydrogel formulations of varying GelMA/m-ELP ratios obtained from the unconfined cyclic compression test. **(c)** Young's modulus and **(d)** maximal extensibility percentage obtained from the tensile test (ns† $p = 0.0887$, ns†† $p = 0.0528$). **(e)** In vitro degradation profiles of the hydrogel samples in 20 µg-collagenase/mL-PBS solution at 37°C. **(f)** Deswelling behavior of the hydrogel samples in saline at 37°C. **(g)** Temperature dependent viscosity profiles of the two selected prepolymer solutions. (* $p < 0.05$, ** $p < 0.01$, *** $p < 0.001$, and **** $p < 0.0001$).

formulations, the pure GelMA sample was first hypothesized to be the ideal artery sealant candidate for the proposed application and an *ex vivo* endovascular anastomosis model was developed for support (Figure 4). However, desired results were not obtained as the anastomosis model failed at an intra-arterial pressure of 12.7 kPa (n = 3, SD = 2.6), which is below normal human systolic blood pressure of 16 kPa. This was due to the previously determined low extensibility (brittleness) of the pure GelMA gel; the anastomosis resulted in cracks within the sealant that lead to leakage. We then introduced the idea of a two-glue system, in which a m-ELP containing formulation with balanced adhesion and elasticity (15/15 composite) would first be

20

applied between two vessels to allow for penetration, followed by an application of the stronger

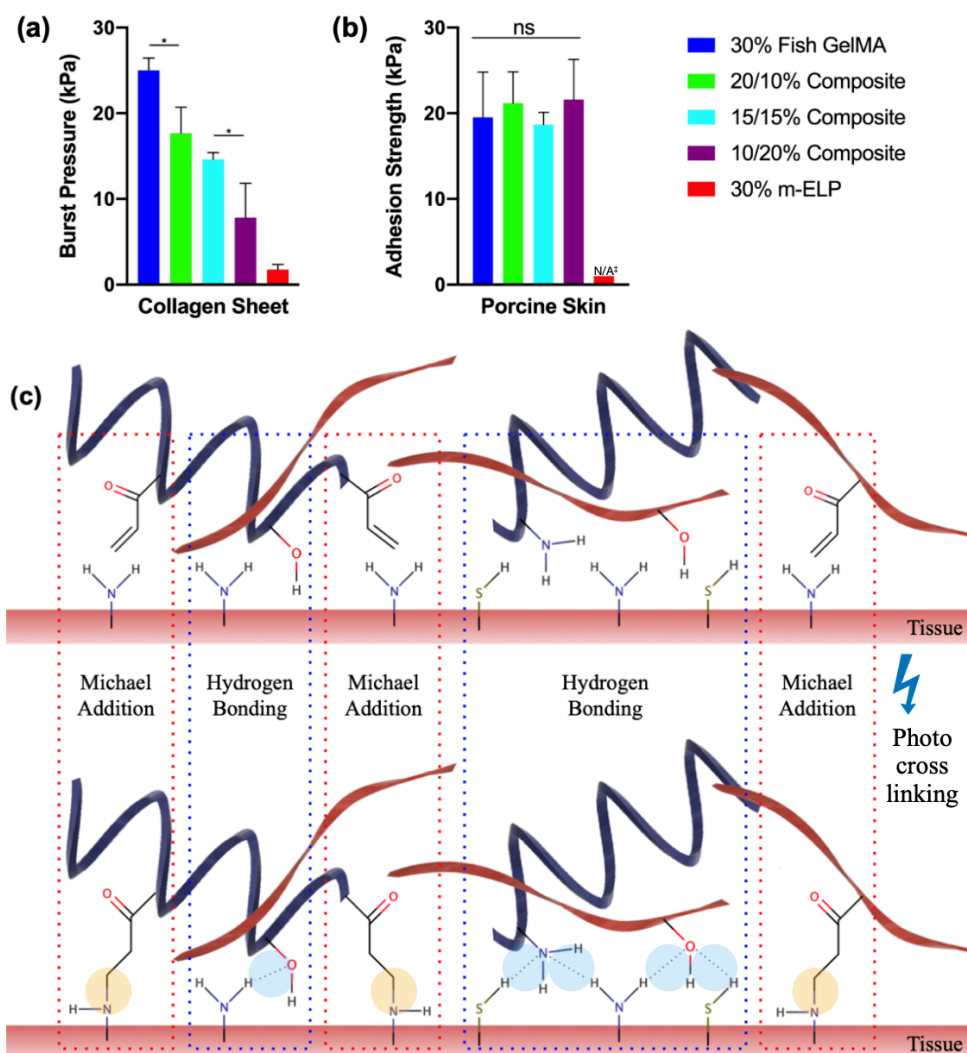GelMA sealant on the sides for further fortification (Figure 4,b).

Fig. 3. Adhesion and cohesion strength of the hydrogel formulations and mechanism of interactions. (a) The *in vitro* burst pressure test provides the relative adhesive strengths of the composites through adhesion to collagen sheet. (b) The wound closure test indicates no difference in cohesive strength between the formulations. ‡The pure m-ELP gel was omitted as it lacks necessary injectability for the precise application of the prepolymer solution for the wound closure test. (c) Schematic of interactions between m-ELP and GelMA polymer chains and tissue before (top) and after (bottom) cross-linking. Two most prominent interactions are covalent linkages and Hydrogen bonding. The covalent linkages are between the methacryloyl alkenes on the polymers and the primary amines on the tissue surface, and form through Michael Addition reactions upon photo-cross-linking when exposed to visible light.

The two-glue system on the same endovascular anastomosis model achieved an intra-arterial pressure of 34.0 kPa (n = 3, SD = 7.5), which is well over normal, elevated, and hypertensive crisis systolic blood pressures in humans at 16, 17.3, and 24 kPa respectively. From this point on, the pure GelMA hydrogel will be referred to as **Glue 1** and the 15:15 GelMA:m-ELP composite as **Glue 2**. The single-glue system was repeated with glue 2 and yielded an even higher burst pressure. However, the significantly faster rate of *in vitro* degradation of glue 2, later confirmed also by the *in vivo* degradation tests, in conjunction with the slow degradation rates desired for the proposed anastomosis procedure underlined the importance of the circumferential application of glue 1. An additional shear test (Figure 4, d) performed using native porcine arteries further showed the enhanced adhesive strength of glue 1 (49.4 kPa, n = 3, SD = 7.0) relative (p = 0.0064) to that of glue 2 (26.7 kPa, n = 3, SD = 5.4).

Cytotoxicity of formulations containing different concentrations of pure GelMA has previously been assessed by our group on various cell types, and GelMA has been shown to be cytocompatible [30, 31]. ELPs have been of particular interest in recent years due to their mechanical properties. However, cell viability has been shown to drop down to as low as 80% with extracellular scaffolds containing ELP and several modifications such as incorporation of fibronectin have been suggested to improve their cytocompatibility [32, 33]. It is critical for glue 2 to allow for high cell proliferation to promote rapid healing of the anastomosis site. Furthermore, we have functionalized ELP with methacryloyl groups (m-ELP) to enhance degree of crosslinking, which could potentially have adverse effects on the cell-material interactions. Therefore, we have performed a 2D cell study using HUVECs to show that glue 2 could
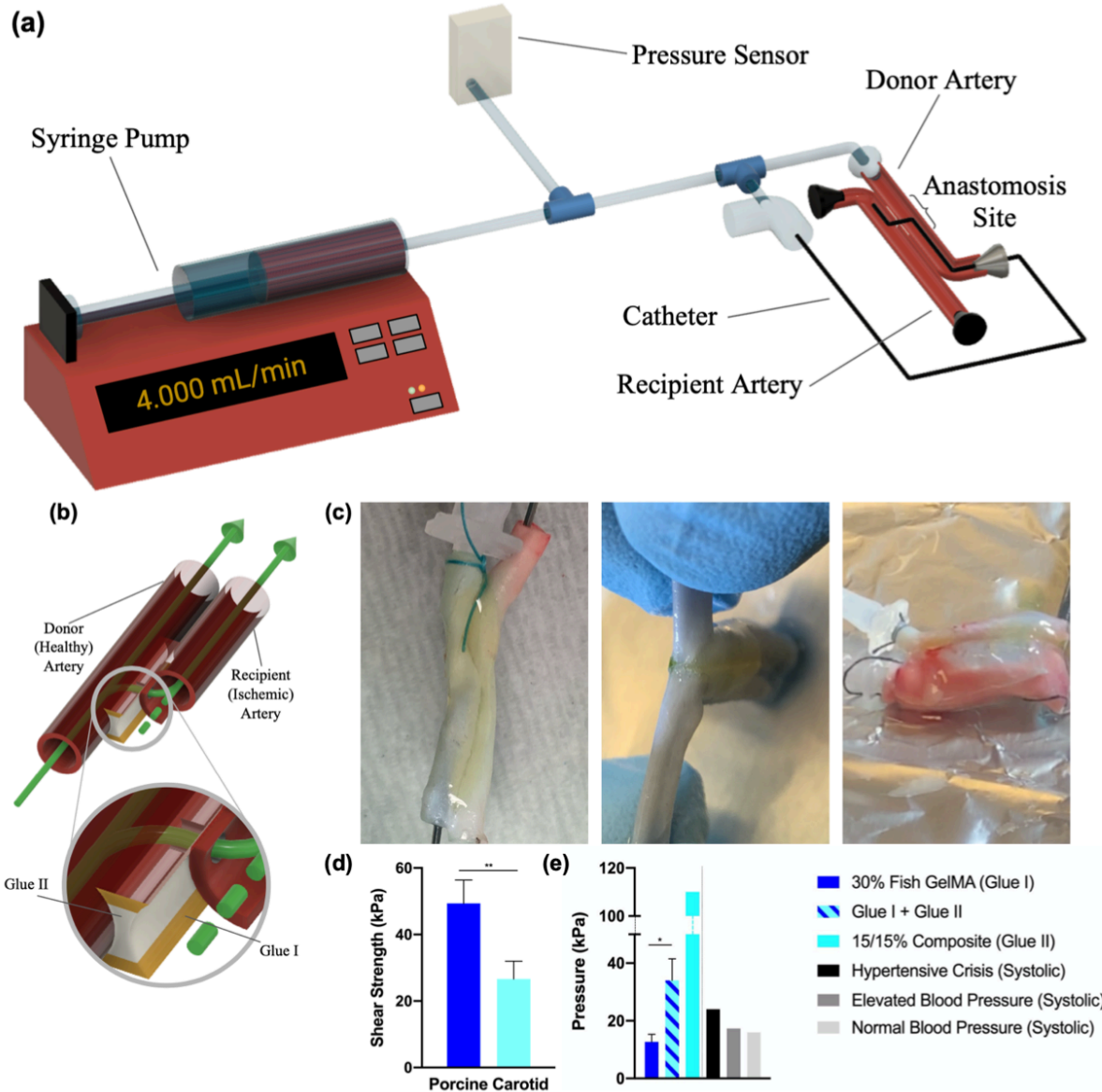
Fig. 4. Ex vivo endovascular anastomosis model and shear test. (a) Experimental setup. **(b)** 3D schematic of the proposed two-glue system. The elastic composite formulation is applied between the arteries to allow penetration through the gel. The rigid pure GelMA formulation is then applied around to stabilize and fortify the anastomosis site. **(c)** Two carotid segments are glued together, the anastomosis procedure is complete and a catheter is inserted (left). The glue seals the area surrounding the anastomosis and prevents fluid leakage, the arteries cannot be pulled apart with ease (center). The burst point during the ex vivo anastomosis model, both arteries expand up to 4-6 times in diameter before the glue system fails and bursts (right). **(d)** Shear strength of the two glues on porcine carotid arteries. **(e)** The maximal intra-arterial pressures achieved with the ex vivo endovascular anastomosis model, in comparison to human systolic blood pressures at various stages.

23

maintain high cell viability and promote cell proliferation. The in vitro cytocompatibility of GelMA/m-ELP composite (glue 2) was evaluated using live/dead and PrestoBlue assays, as well as Actin/DAPI and CD31/DAPI staining. The results demonstrated that glue 2 was capable of supporting proliferation and spreading of the surface seeded, metabolically active HUVECs. The cell viability remained very high (> 97%) during the first 7 days of seeding (Figure 5, a-b).

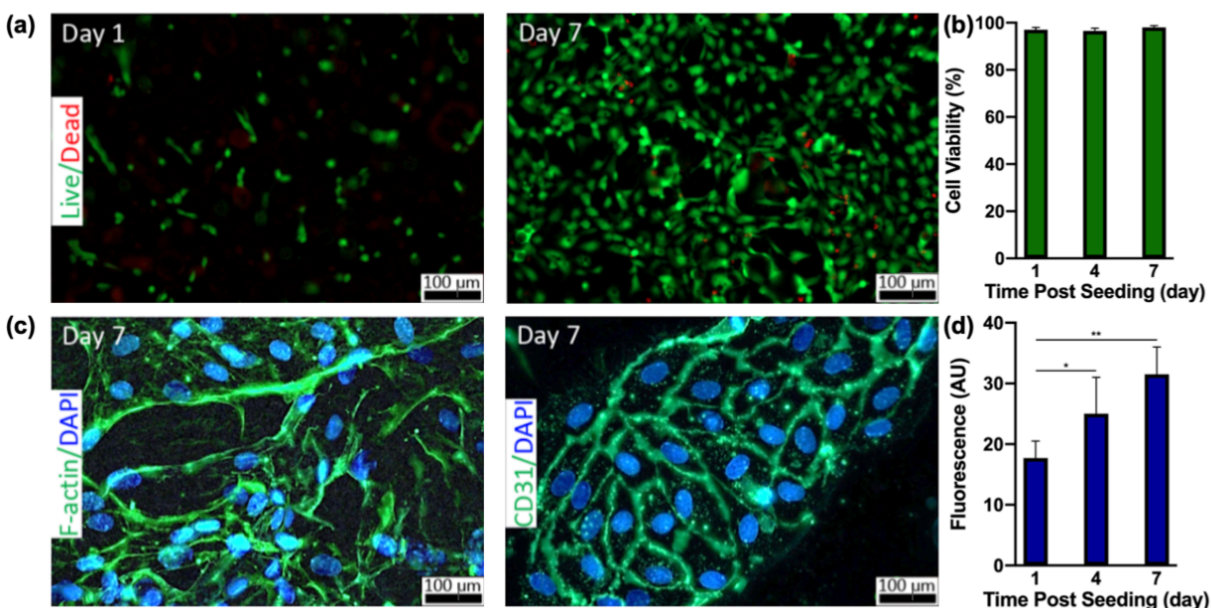**Fig. 5. Cytotoxicity analysis of the composite glue with 2D seeded HUVECs. (a)** Live/dead images show on days 1 through 7 post seeding the viable (green) cells, the non-viable cells (red), the increase in overall cell count, and cell spreading on the surface of the composite hydrogel up to 7 days post seeding. **(b)** The quantification of the live/dead images presents 98 ± 1% cell viability. **(c)** F-actin/DAPI (left) and CD31/DAPI (right) staining on day 7 post seeding show the extensive cell spreading on the surface of the composite hydrogel and the extracellular matrix. **(d)** The PrestoBlue analysis shows a significant increase in fluorescence, thus cell metabolic activity and proliferation on each subsequent time point.

Surface cell density and attachment increased significantly from the first to the seventh day post-seeding (Figure 5, c). In addition, the metabolic activity (fluorescence arbitrary units, a.u.) of HUVECs increased significantly from day 1 (17.7 ± 2.8 a.u.) to day 4 (25.0 ± 6.0 a.u.), and to

24

day 7 (31.5 ± 4.5 a.u.) (Figure 5, d). In short, the live/dead and PrestoBlue assays, as well as the Actin/DAPI and CD31/DAPI staining demonstrate the cytocompatibility of the composite glue.

The *in vivo* degradation profiles of the two selected formulations as well as their immunohistological analysis were studied in a rat subcutaneous implantation model. Hematoxylin/eosin staining of the explanted samples showed a consistent degradation in both samples over the course of the experiment, up to 56 days. (Figure 6, b). While the pure GelMA sample has maintained its overall structural integrity beyond day 28, the 15/15% GelMA/m-ELP composite showed signs of degradation and tissue integration as early as day 7. Furthermore, CD68 and CD3 staining of the sections indicated the infiltration of macrophages and lymphocytes, respectively (Figure 6, d-e). On day 7 post-implantation, there is inflammation around the hydrogel implants, particularly for the 15/15% GelMA/m-ELP composite. However, this initial inflammation can potentially promote wound healing, and subsides significantly with time. The number of immune cells has decreased significantly on days 28 and 56 post-implantation. The *in vivo* degradation profile showed higher degradation rates for the composite gel relative to the pure GelMA sample (Figure 6, c), which supports the *in vitro* degradation results (Figure 2, e).
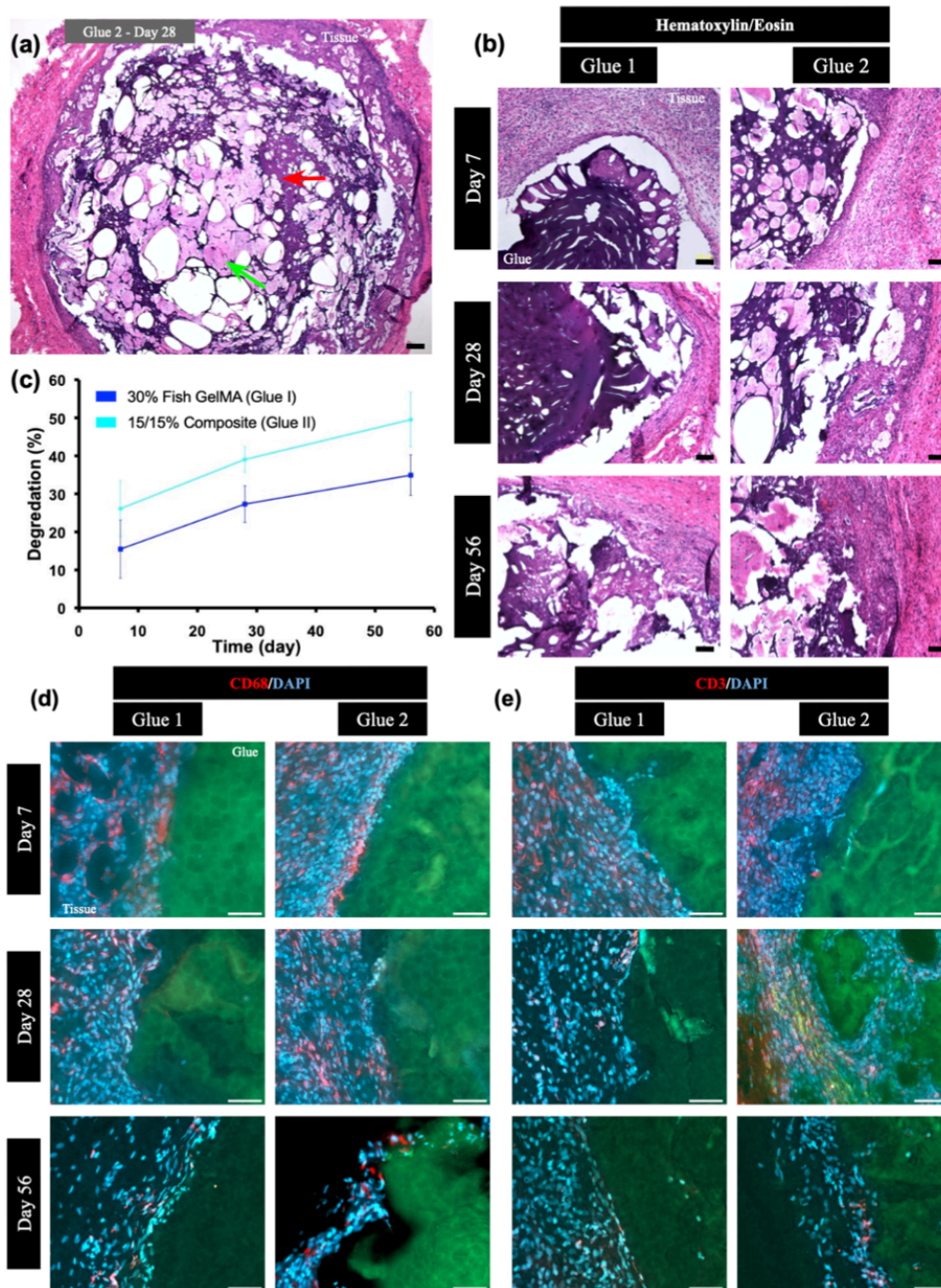
Fig. 6. Immuno-Histological Analysis of the select formulations. (a) Hematoxylin/eosin staining. Degrading hydrogel (red arrow), new tissue integration (green arrow). (Scale bar: 500 μm). **(b)** Hematoxylin/eosin staining of both glue formulations at each time point. For both formulations, the hydrogel is visibly degraded on Day 56 together with tissue integration. (Scale bars: 100 μm). **(c)** The in vivo degradation profiles for both formulations confirm the in vitro findings. **(d-e)** CD68 marker for macrophages and CD3 marker for lymphocytes indicate initial inflammatory response for both formulations that diminishes over time. (Scale bars: 50 μm)

26

The *in vivo* swine model assessed the feasibility of the two-glue sealant as well as the endovascular anastomosis application. The glue was applied and crosslinked at the anastomosis site under homeostatic conditions without difficulty. The anastomosis was created without bleeding complications and then confirmed by x-ray imaging (Figure 7). The procedure was well tolerated. However, malfunction of the Outback needle device in one instance has emphasized the need for novel, purpose-built instruments to create an anastomosis using the intraluminal, transmural approach. Future studies will explore radio frequency ablation for this specific purpose, including how the hydrogel responds to temperature and humidity changes.
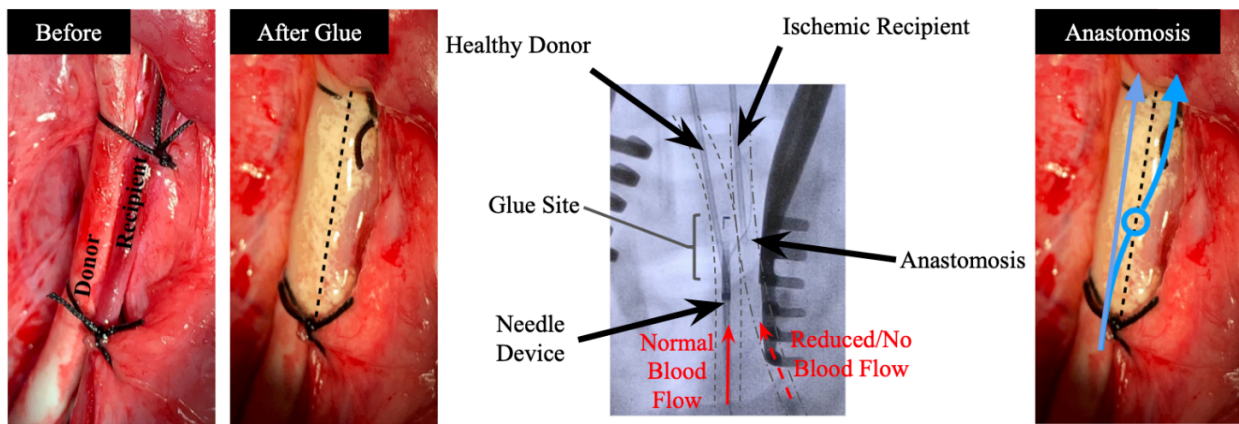

Fig. 7. In vivo pig surgery model. The arteries were tied together with sutures and glued in accordance with the two glue system. The needle device was inserted into the bloodstream from the femoral artery and advanced towards the anastomosis site within the donor artery. A successful anastomosis was performed through the composite glue into the recipient artery.
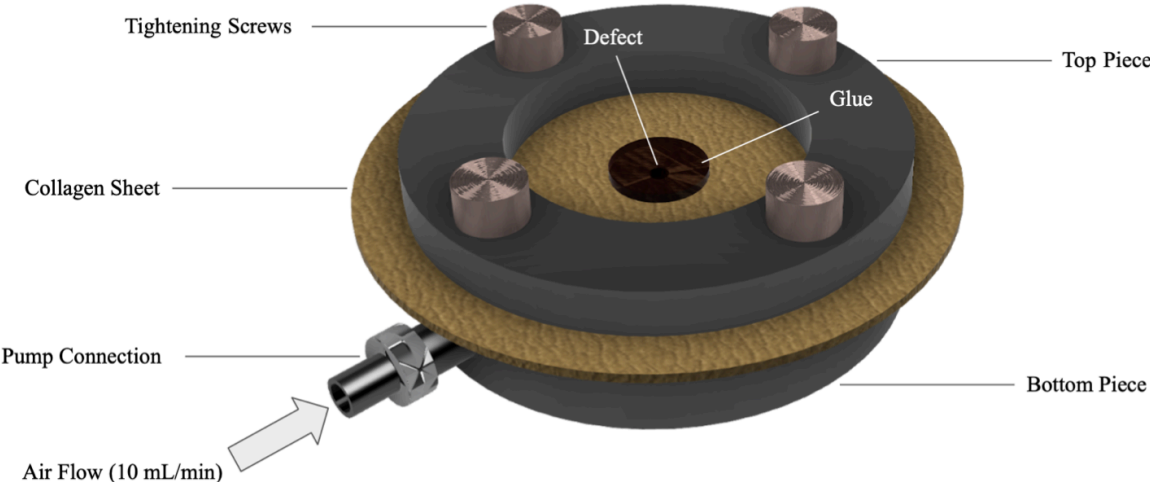
CHAPTER IV. Conclusion

We have modified and characterized m-ELP, a visible light activated recombinant protein that mimics the mechanical properties of natural elastin. This newly developed composite two-glue system exhibited desirable mechanics and biocompatibility in an arterial anastomosis application. The clinical application itself represents a potential alternative to intraluminal stenting or open surgical bypass for the treatment of cerebral ischemia. Additional studies are needed to optimize (i) the size of the anastomosis according to the predetermined parameters unique to each patient and (ii) the rate of glue degradation relative to tissue healing. The former is to ensure sufficient blood flow to both arteries; the latter is critical to maintain the structural integrity of the glue, securing the anastomosis.
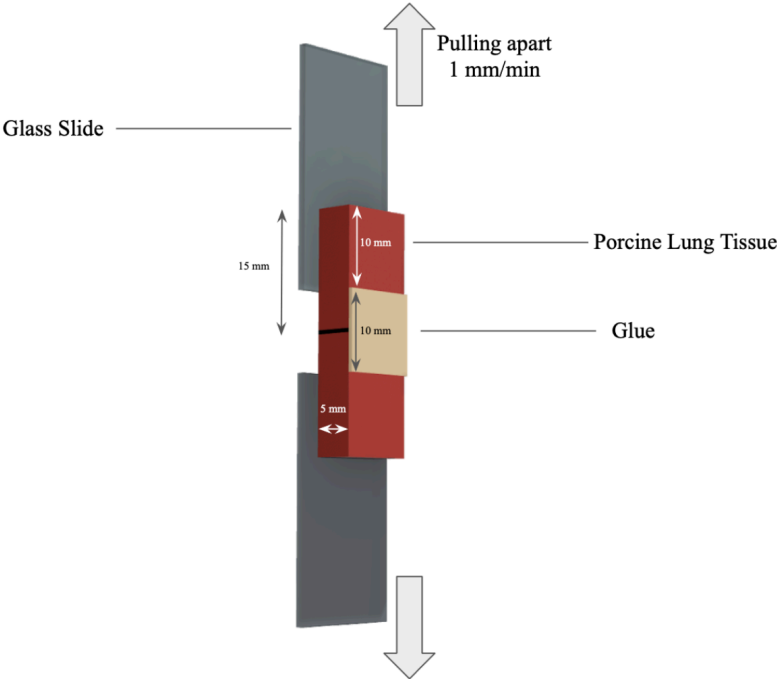
The use of the composite glue we formulated is not limited to the anastomosis application, it can be tuned to be utilized for a broader spectrum. For instance, GelMA/m-ELP hydrogels can serve as sealants with remarkable elasticity and adhesion for vascular or pulmonary defects. Furthermore, the prepolymer solutions can be bioprinted or casted into functionalized scaffolds containing cells or drugs for tissue engineering and drug delivery systems.

Appendices

A1 - Burst Pressure Setup

Tightening Screws
Defect
Top Piece
Glue
Collagen Sheet
Pump Connection
Bottom Piece
Air Flow (10 mL/min)

A2 - Wound Closure Setup

Pulling apart
1 mm/min
Glass Slide
Porcine Lung Tissue
10 mm
Glue
10 mm
15 mm
5 mm

A3 - Shear Setup

Glass Slide

Porcine Carotid
(collapsed)

20 mm

5 mm

Pulling apart
1 mm/min

Side View

Glue
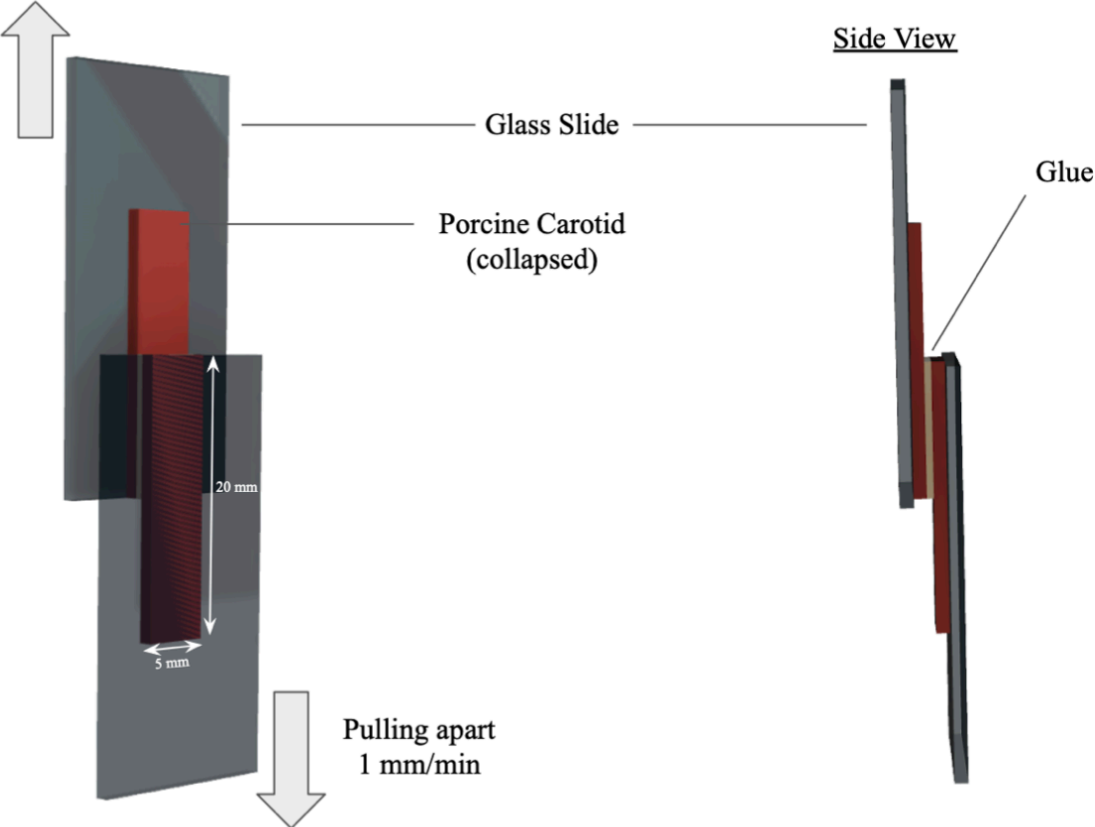
Bibliography

1.   Group, E.I.B.S., Failure of extracranial-intracranial arterial bypass to reduce the risk of ischemic stroke. Results of an international randomized trial. N Engl J Med, 1985. **313**(19): p. 1191-200.

2.   Matsumura, N., et al., Extracranial-intracranial bypass surgery at high magnification using a new high-resolution operating microscope: technical note. Surg Neurol, 2009. **72**(6): p. 690-4.

3.   Steinke, T., J. Rieck, and L. Nuth, Endovascular arteriovenous fistula for hemodialysis access. Gefässchirurgie, 2019. **24**(1): p. 25-31.

4.   *WOUND CLOSURE BIOMATERIALS AND DEVICES*. 2019, [Place of publication not identified: CRC Press.

5.   BIOMATERIALS SCIENCE : an introduction to materials in medicine. 2020, [S.l.]: ELSEVIER ACADEMIC PRESS.

6.   Slaughter, B.V., et al., Hydrogels in regenerative medicine. Adv Mater, 2009. **21**(32-33): p. 3307-29.

7.   Ehrbar, M., et al., Drug-sensing hydrogels for the inducible release of biopharmaceuticals. Nat Mater, 2008. **7**(10): p. 800-4.

8.   Hu, J., et al., A thermo-degradable hydrogel with light-tunable degradation and drug release. Biomaterials, 2017. **112**: p. 133-140.

9.   Liu, X., et al., Ingestible hydrogel device. Nat Commun, 2019. **10**(1): p. 493.

10.   Green, R., Elastic and conductive hydrogel electrodes. Nat Biomed Eng, 2019. **3**(1): p. 9-10.

11.	Hong, Y., et al., A strongly adhesive hemostatic hydrogel for the repair of arterial and heart bleeds. Nat Commun, 2019. **10**(1): p. 2060.

12.	Leong, W., T.T. Lau, and D.A. Wang, A temperature-cured dissolvable gelatin microsphere-based cell carrier for chondrocyte delivery in a hydrogel scaffolding system. Acta Biomater, 2013. **9**(5): p. 6459-67.

13.	Annabi, N., et al., Engineering a highly elastic human protein-based sealant for surgical applications. Sci Transl Med, 2017. **9**(410).

14.	Hewitt, C.W., et al., BioGlue surgical adhesive for thoracic aortic repair during coagulopathy: efficacy and histopathology. Ann Thorac Surg, 2001. **71**(5): p. 1609-12.

15.	Wussler, D., et al., Evaluation of a biocompatible sealant for on-demand repair of vascular defects-a chronic study in a large animal model. Interact Cardiovasc Thorac Surg, 2020. **30**(5): p. 715-723.

16.	Vyas, K.S. and S.P. Saha, Comparison of hemostatic agents used in vascular surgery. Expert Opin Biol Ther, 2013. **13**(12): p. 1663-72.

17.	Peppas, N.A., et al., Hydrogels in Biology and Medicine: From Molecular Principles to Bionanotechnology. Advanced Materials, 2006. **18**(11): p. 1345-1360.

18.	Ghosh, S., et al., Strong poly(ethylene oxide) based gel adhesives via oxime cross-linking. Acta Biomater, 2016. **29**: p. 206-214.

19.	Bichara, D.A., et al., Porous poly(vinyl alcohol)-hydrogel matrix-engineered biosynthetic cartilage. Tissue Eng Part A, 2011. **17**(3-4): p. 301-9.

20.	Zhang, Z., et al., Biodegradable and thermoreversible PCLA-PEG-PCLA hydrogel as a barrier for prevention of post-operative adhesion. Biomaterials, 2011. **32**(21): p. 4725-36.

21.   Schloss, A.C., D.M. Williams, and L.J. Regan, *Protein-Based Hydrogels for Tissue Engineering.* Adv Exp Med Biol, 2016. **940**: p. 167-177.

22.   Zhang, Y.N., et al., A Highly Elastic and Rapidly Crosslinkable Elastin-Like Polypeptide-Based Hydrogel for Biomedical Applications. Adv Funct Mater, 2015. **25**(30): p. 4814-4826.

23.   Van Den Bulcke, A.I., et al., Structural and rheological properties of methacrylamide modified gelatin hydrogels. Biomacromolecules, 2000. **1**(1): p. 31-8.

24.   Yue, K., et al., Structural analysis of photocrosslinkable methacryloyl-modified protein derivatives. Biomaterials, 2017. **139**: p. 163-171.

25.   Claassen, C., et al., Quantification of Substitution of Gelatin Methacryloyl: Best Practice and Current Pitfalls. Biomacromolecules, 2018. **19**(1): p. 42-52.

26.   Cardiff, R.D., C.H. Miller, and R.J. Munn, Manual hematoxylin and eosin staining of mouse tissue sections. Cold Spring Harb Protoc, 2014. **2014**(6): p. 655-8.

27.   Annabi, N., et al., Engineering a sprayable and elastic hydrogel adhesive with antimicrobial properties for wound healing. Biomaterials, 2017. **139**: p. 229-243.

28.   Shirzaei Sani, E., et al., Engineering Adhesive and Antimicrobial Hyaluronic Acid/ Elastin-like Polypeptide Hybrid Hydrogels for Tissue Engineering Applications. ACS Biomaterials Science & Engineering, 2018. **4**(7): p. 2528-2540.

29.   Yin, J., et al., 3D Bioprinting of Low-Concentration Cell-Laden Gelatin Methacrylate (GelMA) Bioinks with a Two-Step Cross-linking Strategy. ACS Appl Mater Interfaces, 2018. **10**(8): p. 6849-6857.

30.   Noshadi, I., et al., In vitro and in vivo analysis of visible light crosslinkable gelatin methacryloyl (GelMA) hydrogels. Biomater Sci, 2017. **5**(10): p. 2093-2105.

31.   Fares, M.M., et al., Interpenetrating network gelatin methacryloyl (GelMA) and pectin-g-PCL hydrogels with tunable properties for tissue engineering. Biomater Sci, 2018. **6**(11): p. 2938-2950.

32.   Ravi, S., et al., Incorporation of fibronectin to enhance cytocompatibility in multilayer elastin-like protein scaffolds for tissue engineering. J Biomed Mater Res A, 2013. **101**(7): p. 1915-25.

33.   Le, D.H.T., et al., Double-hydrophobic elastin-like polypeptides with added functional motifs: Self-assembly and cytocompatibility. J Biomed Mater Res A, 2017. **105**(9): p. 2475-2484.